Available online at www.sciencedirect.com
SCIENCE DIRECT®
Journal of Sound and Vibration 276 (2004) 1–11
JOURNAL OF SOUND AND VIBRATION
www.elsevier.com/locate/jsvi

A comparative study on time–frequency feature of cracked rotor by Wigner–Ville distribution and wavelet transform

J. Zou*, J. Chen

The State Key Laboratory of Vibration, Shock & Noise, Shanghai Jiao Tong University, 1954 Huashan Road, Shanghai 200030, People's Republic of China

Received 23 July 2002; accepted 14 July 2003

Abstract

Based on the simple hinge crack model, the dynamic equation of transient response in a cracked rotor system is modelled; the numerical simulation solutions of the cracked rotor and the uncracked rotor are obtained from the model. The time–frequency features of the cracked and the uncracked rotors obtained by using the Wigner–Ville distribution are compared with those obtained by using the wavelet transform, the difference is presented. By simulation research, the sensitivity of the Wigner–Ville distribution and the wavelet transform to the stiffness variation is investigated; and the influence of the unbalance and the unbalance angle on the Wigner–Ville distribution and the wavelet transform is discussed. The time–frequency features are unique, which can be used as the criteria for identification of cracked rotor.

1. Introduction

Dynamic behaviors of the cracked rotor have been observed since the 1970s, and the corresponding dynamic analysis has been investigated for the last three decades [1–3].

In 1976, Gasch [3,4] proposed a simple hinge crack model that was very good for the representation of the cyclic stiffness variables and the stability limits. Dimarogonas and his colleagues [5–7] derived a rough analytical estimation of the crack compliance based on the energy principle of Paris. The research of Gasch and Dimarogonas is adopted by many of the following papers; however, most of the following research is involved in the cracked rotor rotating at a constant speed, and the research on transient response of the cracked rotor has been limited. Ratan [8,9] studied the transient response characteristics using SMAC techniques. Plaut [10] discussed the behavior of a cracked rotating shaft by using Galerkin's method and numerical

*Corresponding author.
E-mail address: jianzou@sjtu.edu.cn (J. Zou).

0022-460X/$ - see front matter © 2003 Published by Elsevier Ltd.
doi:10.1016/j.jsv.2003.07.002

integration. Sekhar and Prabhu [11,12] made transient analysis of a cracked rotor passage through critical speed; based on the research of Sekhar, Prabhakar [13] investigated the detection and monitoring of cracks in a rotor–bearing system using wavelet transforms. Zou [14] presented the time–frequency features of the cracked and the uncracked rotors by wavelet transform. Now, there is extensive research on the vibrational behavior of cracked shaft and the use of response characteristics to detect crack. But from the viewpoint of engineering practices, the identification of the cracked rotor is still at the stage of theoretical research for the deficiency of the traditional signal processing methods in non-stationary signal.

The Wigner–Ville distribution and wavelet transform are widely used in the field of time–frequency feature extraction, which are very powerful and appealing tools for the analysis of non-stationary, non-linear and transient signals [15–21]. However, to the best of the authors' knowledge, there is no work reported on the application of the Wigner–Ville distribution to identification of cracked rotor, and the research on the wavelet time–frequency feature of the cracked rotor is few.

In the present study, the dynamic equation of transient response in a cracked system is modelled. The time–frequency features of the cracked rotor and the uncracked rotor obtained by using the Wigner–Ville distribution are compared with those obtained by using the wavelet transform. By simulation research, the sensitivity of the Wigner–Ville distribution and the wavelet transform to the stiffness variation is investigated; and the influence of the unbalance and the unbalance angle on the Wigner–Ville distribution and the wavelet transform is discussed.

2. Dynamic model and numerical solutions

Consider a de Laval rotor with a disc mass m supported by a massless elastic shaft of length L. Suppose that the crack is located near the disc and the weight is dominant, the dynamic equation of the cracked rotor (shown in Fig. 1) can be written as

$$\begin{bmatrix} m & 0 \\ 0 & m \end{bmatrix} \begin{pmatrix} \ddot{x} \\ \ddot{y} \end{pmatrix} + \begin{bmatrix} c & 0 \\ 0 & c \end{bmatrix} \begin{pmatrix} \dot{x} \\ \dot{y} \end{pmatrix} + \begin{bmatrix} k_x & k_{xy} \\ k_{yx} & k_y \end{bmatrix} \begin{pmatrix} x \\ y \end{pmatrix} = \begin{pmatrix} F_x \\ F_y \end{pmatrix} + \begin{pmatrix} mg \\ 0 \end{pmatrix}, \tag{1}$$

where c is the damping coefficient.

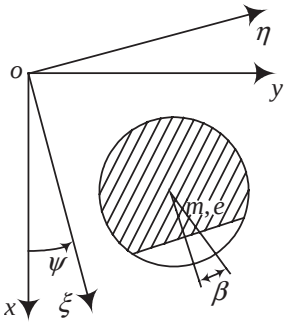

Fig. 1. The cross-section of the cracked rotor.

The stiffness matrix in the inertial frame can be obtained from the stiffness matrix in the rotational frame by transformation matrix. The stiffness matrix in the rotational frame is as follows:

$$\begin{bmatrix} k_\xi & \\ & k_\eta \end{bmatrix} = \begin{bmatrix} k & \\ & k \end{bmatrix} - \Theta \begin{bmatrix} \Delta k_\xi & \\ & 0 \end{bmatrix}, \tag{2}$$

where k_ξ is the stiffness in the ξ-axis direction, k_η is the stiffness in the η-axis direction, k is the stiffness of the uncracked rotor, Δk_ξ is the stiffness variation in the ξ-axis direction.

As the weight is dominant, the modified function Θ of the opening and closing of the crack can be written as

$$\Theta = \begin{cases} 1 & 2k\pi \leqslant \theta < (2k+\frac{1}{2})\pi \quad \text{the crack is open,} \\ 0 & (2k+\frac{1}{2})\pi \leqslant \theta < (2k+\frac{3}{2})\pi \quad \text{the crack is closed,} \\ 1 & (2k+\frac{3}{2})\pi \leqslant \theta < (2k+2)\pi \quad \text{the crack is open,} \end{cases} \tag{3}$$

where $k = 0, 1, 2, \ldots$, $\theta = \frac{1}{2}a_1 t^2 + \omega_0 t + \beta$, a_1 is the angular acceleration, ω_0 is the initial angular speed, β is the angle of the unbalance with respect to the ξ-axis.

By Fourier transform, the modified function is changed into

$$\Theta = \frac{1}{2} + \frac{2}{\pi}\cos\theta - \frac{2}{3\pi}\cos 3\theta + \frac{2}{5\pi}\cos 5\theta - \cdots. \tag{4}$$

From Fig. 1, the transformation matrix is

$$\mathbf{T} = \begin{bmatrix} \cos\psi & \sin\psi \\ -\sin\psi & \cos\psi \end{bmatrix},$$

where $\psi = \frac{1}{2}a_1 t^2 + \omega_0 t$.

The stiffness matrix in the inertial frame can be written as

$$\begin{bmatrix} k_x & k_{xy} \\ k_{yx} & k_y \end{bmatrix} = \mathbf{T}^{-1} \begin{bmatrix} k_\xi & \\ & k_\eta \end{bmatrix} \mathbf{T} = \begin{bmatrix} k & 0 \\ 0 & k \end{bmatrix} - \Theta \Delta k_\xi \begin{bmatrix} \cos^2\psi & \sin\psi\cos\psi \\ \sin\psi\cos\psi & \sin^2\psi \end{bmatrix}. \tag{5}$$

The excitation forces F_x, F_y are given as

$$\begin{pmatrix} F_x \\ F_y \end{pmatrix} = me \begin{pmatrix} \ddot{\theta}\sin\theta + \dot{\theta}^2\cos\theta \\ -\ddot{\theta}\cos\theta + \dot{\theta}^2\sin\theta \end{pmatrix}, \tag{6}$$

where e is the eccentricity of the disc.

Introducing the dimensionless variables

$$\tau = \omega_n \cdot t, \quad \Omega_0 = \frac{\omega_0}{\omega_n}.$$

Eq. (1) is transformed into the dimensionless form

$$\begin{pmatrix} x_{\tau\tau}/x_{st} \\ y_{\tau\tau}/x_{st} \end{pmatrix} + \begin{bmatrix} 2\zeta & 0 \\ 0 & 2\zeta \end{bmatrix} \begin{pmatrix} x_{\tau}/x_{st} \\ y_{\tau}/x_{st} \end{pmatrix} + \begin{pmatrix} x/x_{st} \\ y/x_{st} \end{pmatrix} = \begin{pmatrix} 1 \\ 0 \end{pmatrix} + \Theta \Delta_{k_\xi} \begin{bmatrix} \cos^2\psi & \sin\psi\cos\psi \\ \sin\psi\cos\psi & \sin^2\psi \end{bmatrix}$$
$$\begin{pmatrix} x/x_{st} \\ y/x_{st} \end{pmatrix} + \varepsilon \begin{bmatrix} a_r \sin\left(\frac{1}{2}a_r\tau^2 + \Omega_0\tau + \beta\right) + (a_r\tau + \Omega_0)^2 \cos\left(\frac{1}{2}a_r\tau^2 + \Omega_0\tau + \beta\right) \\ -a_r \cos\left(\frac{1}{2}a_r\tau^2 + \Omega_0\tau + \beta\right) + (a_r\tau + \Omega_0)^2 \sin\left(\frac{1}{2}a_r\tau^2 + \Omega_0\tau + \beta\right) \end{bmatrix}, \tag{7}$$

where the subscript τ and the double subscript $\tau\tau$ mean the first and the second derivative with respect to τ, $\omega_n = \sqrt{k/m}$ is the natural frequency, $\zeta = c/2m\omega_n$ is the damping ratio, $x_{st} = mg/k$ is the static deflection, $\varepsilon = e/x_{st}$ is the relative eccentricity, $\Delta_{k_\xi} = \Delta k_\xi/k$ is the relative stiffness variation, $a_r = a_1/\omega_n^2$ is the relative angular acceleration. In Eq. (7), the second term on the right-hand side denotes the crack excitation.

If weight dominance is assumed, the equation is satisfied as follows [3,4]:

$$\begin{pmatrix} x \\ y \end{pmatrix} \approx \begin{pmatrix} x \\ y \end{pmatrix}_{st} = \begin{pmatrix} \frac{mg}{k} \\ 0 \end{pmatrix} = \begin{pmatrix} x_{st} \\ 0 \end{pmatrix}.$$

Eq. (7) is rewritten as

$$\begin{aligned} &\begin{pmatrix} x_{\tau\tau}/x_{st} \\ y_{\tau\tau}/x_{st} \end{pmatrix} + \begin{bmatrix} 2\zeta & 0 \\ 0 & 2\zeta \end{bmatrix} \begin{pmatrix} x_{\tau}/x_{st} \\ y_{\tau}/x_{st} \end{pmatrix} + \begin{pmatrix} x/x_{st} \\ y/x_{st} \end{pmatrix} \\ &\quad = \begin{pmatrix} 1 \\ 0 \end{pmatrix} + \Theta \Delta_{k_\xi} \begin{bmatrix} \cos^2\psi & \sin\psi\cos\psi \\ \sin\psi\cos\psi & \sin^2\psi \end{bmatrix} \\ &\quad \times \begin{pmatrix} 1 \\ 0 \end{pmatrix} + \varepsilon \begin{bmatrix} a_r \sin\left(\frac{1}{2}a_r\tau^2 + \Omega_0\tau + \beta\right) + (a_r\tau + \Omega_0)^2 \cos\left(\frac{1}{2}a_r\tau^2 + \Omega_0\tau + \beta\right) \\ -a_r \cos\left(\frac{1}{2}a_r\tau^2 + \Omega_0\tau + \beta\right) + (a_r\tau + \Omega_0)^2 \sin\left(\frac{1}{2}a_r\tau^2 + \Omega_0\tau + \beta\right) \end{bmatrix}. \end{aligned} \tag{8}$$

Applying state space notation, Eq. (8) is rewritten as

$$\dot{\mathbf{X}} = \mathbf{A}\mathbf{X} + \mathbf{F}, \tag{9}$$

where $\mathbf{X}$ denotes the four-dimensional state vector

$$\mathbf{X} = \begin{pmatrix} x_{\tau}/x_{st} \\ y_{\tau}/x_{st} \\ x/x_{st} \\ y/x_{st} \end{pmatrix},$$

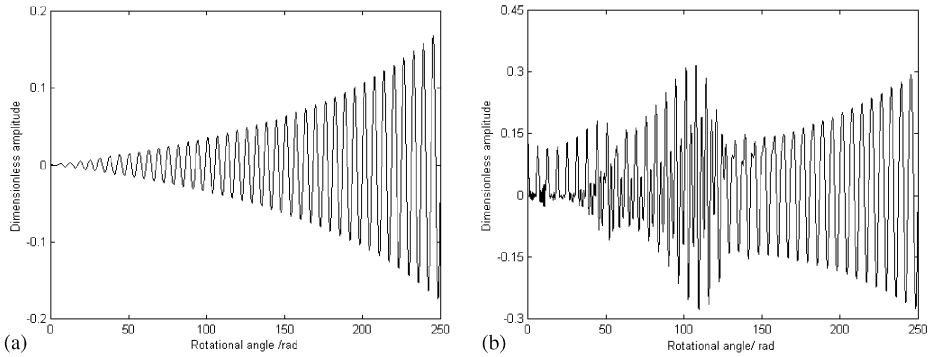

Fig. 2. Time waveform of the uncracked rotor (a) and the cracked rotor (b).

A is the 4×4 system matrix

$$\mathbf{A} = \begin{pmatrix} -2\zeta & 0 & -1 & 0 \\ 0 & -2\zeta & 0 & -1 \\ 1 & 0 & 0 & 0 \\ 0 & 1 & 0 & 0 \end{pmatrix},$$

F is the four-dimensional vector of excitation functions.

By using classical Runge–Kutta method, the dynamic response is obtained on the condition that the weight is neglected in order to erase the influence of the static component of the response due to the weight on the time–frequency features of the rotors. Let $a_r = 0.0013, \Omega_0 = 0$, $\varepsilon = 0.1, \Delta_{k_\xi} = 0.1, \beta = 0, \zeta = 0.05$, the numerical solutions of the cracked rotor and the uncracked rotor are shown in Fig. 2. From Fig. 2, the sub-harmonic resonance of the transient response passage through $\frac{1}{3}$ or $\frac{1}{2}$ sub-critical speed in the cracked rotor system is obvious; and there is no sub-harmonic resonance in the unbalanced rotor.

3. Time–frequency feature investigation

3.1. Basic theory

The wavelet time–frequency transform is multi-resolution analysis algorithm, which is the inner product of the signal and a family of the wavelet. For the mother wavelet or the wavelet prototype $\psi(t)$, there is the corresponding family of the wavelet, which is called the son wavelet. The series of the son wavelets are generated by the dilation and translation from the mother wavelet $\psi(t)$ as follows:

$$\psi_{a,b}(t) = \frac{1}{\sqrt{|a|}} \psi\left(\frac{t-b}{a}\right), \tag{10}$$

where a is scale factor, b is time shift, the factor $|a|^{-1/2}$ is used to ensure energy preservation.

The mother wavelet $\psi(t)$ is considered to be the square integrable complex function, it must satisfy the admissibility condition

$$c_\psi = \int_{-\infty}^{+\infty} \frac{|\psi(\omega)|^2}{|\omega|} \mathrm{d}\omega < \infty,$$

where $\psi(\omega)$ is the Fourier transform of $\psi(t)$.

The continuous wavelet time–frequency transform of the initial signal $s(t)$ can be written as

$$W_s(a,b) = \int s(t) \cdot \psi^*_{a,b}(t)\, \mathrm{d}t, \tag{11}$$

where $\psi^*_{a,b}(t)$ is the complex conjugate function of $\psi_{a,b}(t)$.

With the variation of scale factor a and time shift b, the wavelet time–frequency transform coefficients $W_s(a,b)$ are obtained. Due to the variation of scale factor a and time shift b, the wavelet time–frequency transform coefficients $W_s(a,b)$ can offer the representation of the signal $s(t)$ at different levels of resolution and time shift, thus the wavelet time–frequency transform can be used to extract the features of the signal $s(t)$.

The continuous Wigner–Ville distribution of the initial signal $s(t)$ can be written as

$$W_z(t,f) = \int_{-\infty}^{+\infty} z\left(t+\frac{\tau}{2}\right) z^*\left(t-\frac{\tau}{2}\right) e^{-\mathrm{j}2\pi\tau f}\, \mathrm{d}\tau, \tag{12}$$

where * denotes complex conjugation, $z(t)$ is the analytical signal of the initial signal $s(t)$.

The Wigner–Ville distribution is a two-dimensional function that maps a one-dimensional time function $s(t)$ into a time and frequency plane, so the Wigner–Ville distribution can be used to represent the time–frequency features of the cracked and the uncracked rotors.

3.2. Comparison Wigner–Ville distribution with wavelet transform

Let $a_r = 0.0013$, $\Omega_0 = 0$, $\varepsilon = 0.1$, $\beta = 0$, $\zeta = 0.05$, $\Delta_{k_\xi} = 0, 0.1$, the numerical simulation solutions of the cracked rotor and the uncracked rotor passage through $\frac{1}{3}$ subcritical speed are obtained. The data between the rotational angle $\psi = 44.08$ and 50.35 rad are sampled, and the sampling interval τ_s is 0.14 rad. The sampled data are processed by Wigner–Ville distribution and

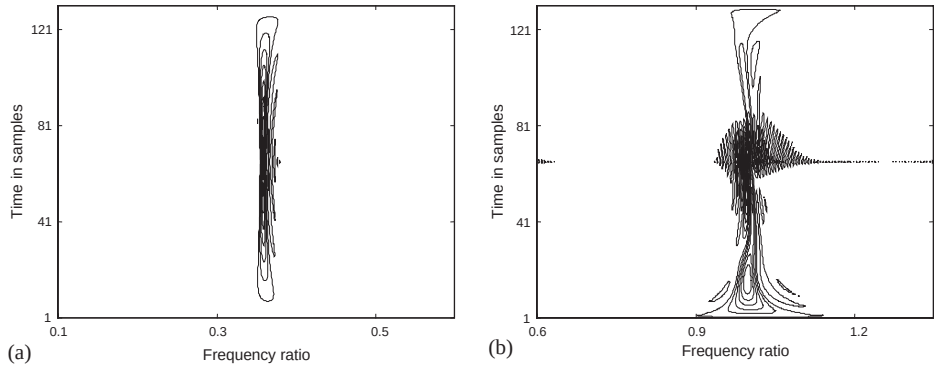

Fig. 3. Wigner–Ville time–frequency features of the uncracked rotor (a) and the cracked rotor (b).

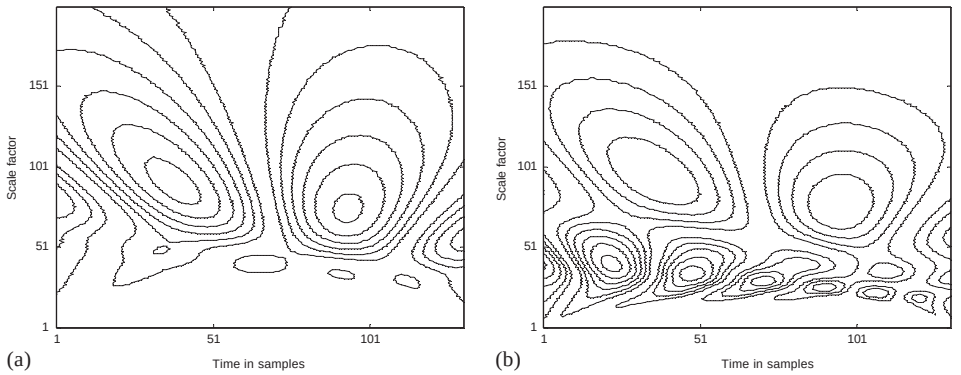

Fig. 4. Wavelet time–frequency features of the uncracked rotor (a) and the cracked rotor (b).

Daubechies 10 wavelet, and the Wigner–Ville time–frequency features and the wavelet time–frequency features of the cracked and the uncracked rotors are shown in Figs. 3 and 4.

From Fig. 3, the Wigner–Ville time–frequency features of the cracked and the uncracked rotors are different. The Wigner–Ville time–frequency feature of the uncracked rotor takes on the form of regular ellipses under the influence of the unbalance, and the frequency components are in the range of [0.3–0.35] corresponding to the frequency components of the unbalance. For the cracked rotor, the crack excitation results in oscillation in the Wigner–Ville time–frequency feature, which corresponds to the sub-harmonic resonance of the cracked rotor; and the frequency components become complex, which are about in the range of [1.0–1.2] corresponding to the third harmonic of the crack excitation. So the Wigner–Ville time–frequency features can be used to identify the cracked rotor and the uncracked rotor.

In Fig. 4, the wavelet time–frequency features of the cracked and the uncracked rotors are in different form. The two-dimensional wavelet spectrum of the uncracked rotor is characteristic of two group circles due to the unbalance, the variation of time shift and scale factor, however, the two-dimensional wavelet spectrum of the cracked rotor is characteristic of six group circles that result from the third harmonic of the crack excitation, the variation of time shift and scale factor besides two group circles due to the unbalance. The wavelet time–frequency features of the cracked and the uncracked rotors are distinct, which can be used to identify the cracked rotor.

Comparing Fig. 3 with Fig. 4, the conclusion is that the wavelet transform and the Wigner–Ville distribution can identify the cracked rotor effectively. But the difference of the time–frequency features between the cracked and the uncracked rotors obtained by wavelet transform is more obvious than that obtained by Wigner–Ville distribution, so to some extent, the wavelet transform is superior to the Wigner–Ville distribution.

4. Comparision of sensitivity to the stiffness variation

The presence of a crack tends to decrease the stiffness, and the dynamic response varies with the stiffness variation. Let $a_r = 0.0013$, $\Omega_0 = 0$, $\varepsilon = 0.1$, $\beta = 0$, $\zeta = 0.05$, $\Delta_{k_\xi} = 0.01$ and $\Delta_{k_\xi} = 0.02$ to investigate the sensitivity of the Wigner–Ville distribution and the wavelet transform to the stiffness variation, the results are shown in Figs. 5 and 6. It can be seen from Figs. 5 and 6 that the

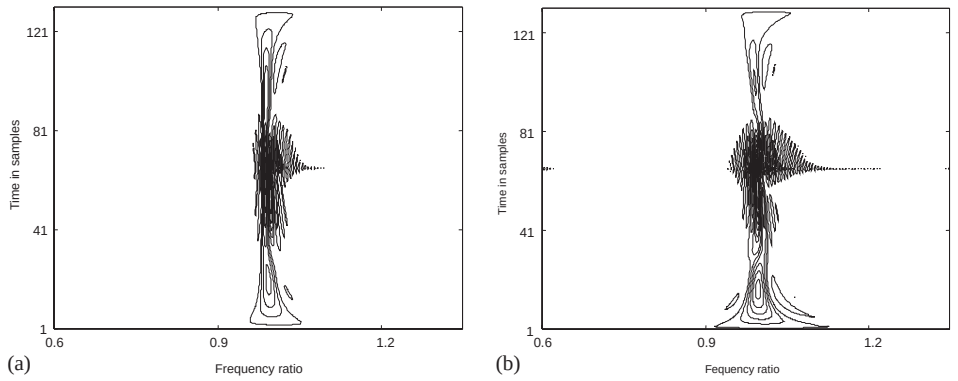

Fig. 5. Sensitivity of Wigner–Ville distribution to the stiffness variation: (a) $\Delta_{k_\xi} = 0.01$, (b) $\Delta_{k_\xi} = 0.02$.

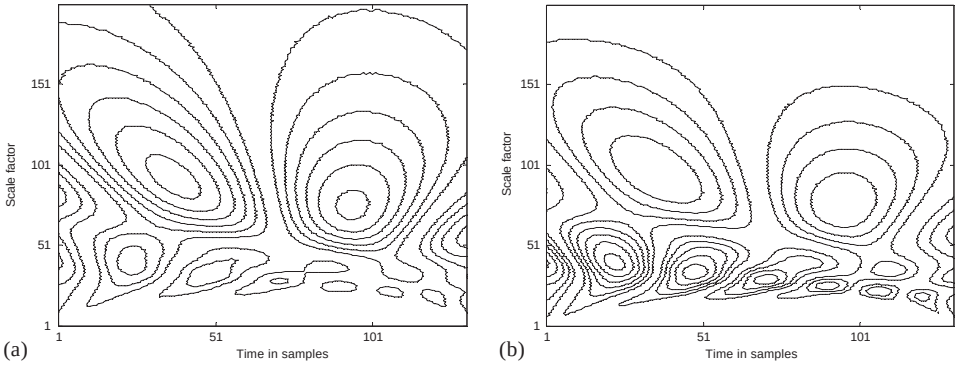

Fig. 6. Sensitivity of wavelet transform to the stiffness variation: (a) $\Delta_{k_\xi} = 0.01$, (b) $\Delta_{k_\xi} = 0.02$.

wavelet transform is more sensitive to the stiffness variation than the Wigner–Ville distribution; even if the stiffness variation is only 1%, the wavelet transform still can identify the cracked rotor.

5. Comparison of the influence of system parameters

5.1. The influence of the unbalance

Let $a_r = 0.0013$, $\Omega_0 = 0$, $\Delta_{k_\xi} = 0.1$, $\beta = 0$, $\zeta = 0.05$, $\varepsilon = 0.2$ and $\varepsilon = 0.3$ to investigate the influence of the unbalance on the Wigner–Ville time–frequency feature and the wavelet time–frequency feature. As it is shown in Figs. 7 and 8, even if the unbalance increases significantly, the Wigner–Ville distribution and the wavelet transform still can identify the cracked rotor effectively.

5.2. The influence of the unbalance angle

Let $a_r = 0.0013$, $\Omega_0 = 0$, $\Delta_{k_\xi} = 0.1$, $\varepsilon = 0.1$, $\zeta = 0.05$, $\beta = \pi/2$ and $\beta = \pi$ to investigate the influence of the unbalance angle on the Wigner–Ville time–frequency feature and the wavelet time–frequency feature (Figs. 9 and 10). By comparison of Fig. 9 with Fig. 3, the conclusion is

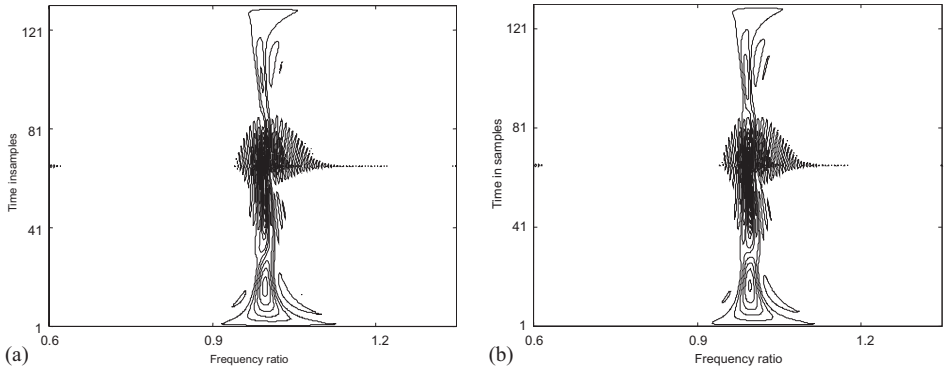

Fig. 7. The influence of the unbalance on Wigner–Ville time–frequency feature: (a) $\varepsilon = 0.2$, (b) $\varepsilon = 0.3$.

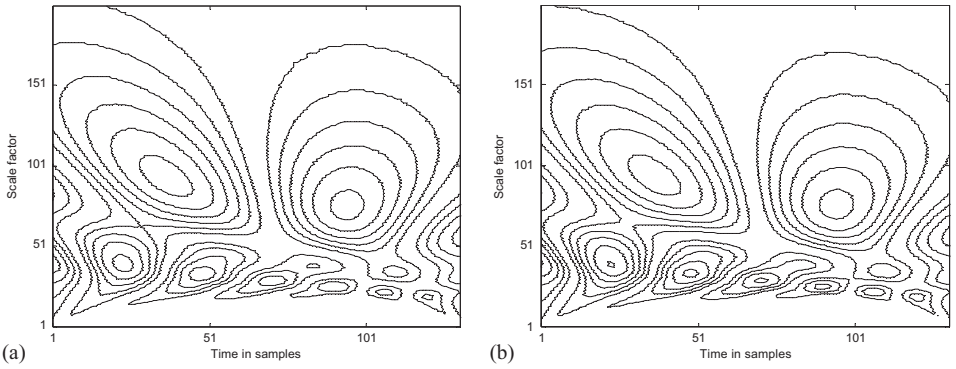

Fig. 8. The influence of the unbalance on wavelet time–frequency feature: (a) $\varepsilon = 0.2$, (b) $\varepsilon = 0.3$.

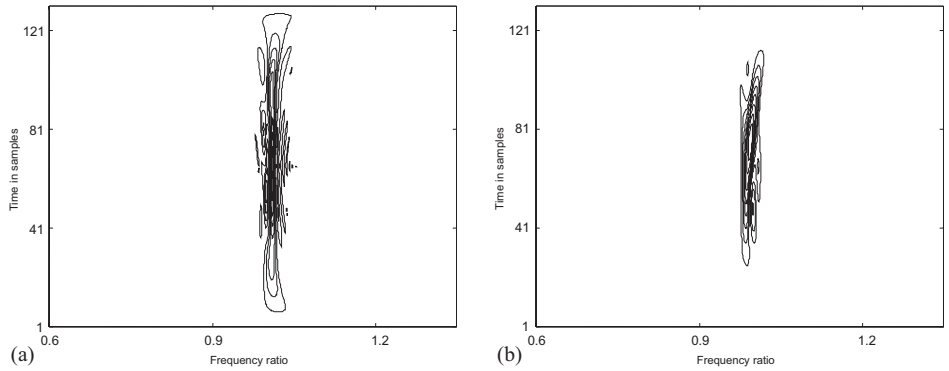

Fig. 9. The influence of the unbalance angle on the Wigner–Ville time–frequency feature: (a) $\beta = \pi/2$, (b) $\beta = \pi$.

drawn that the influence of the unbalance angle on the Wigner–Ville time–frequency feature is great, when $\beta = \pi/2$ or π, the oscillation of the Wigner–Ville time–frequency feature becomes weak so that the cracked rotor cannot be identified effectively. Compared with Fig. 4, Fig. 10 shows that the influence of the unbalance angle on the wavelet time–frequency feature is small,

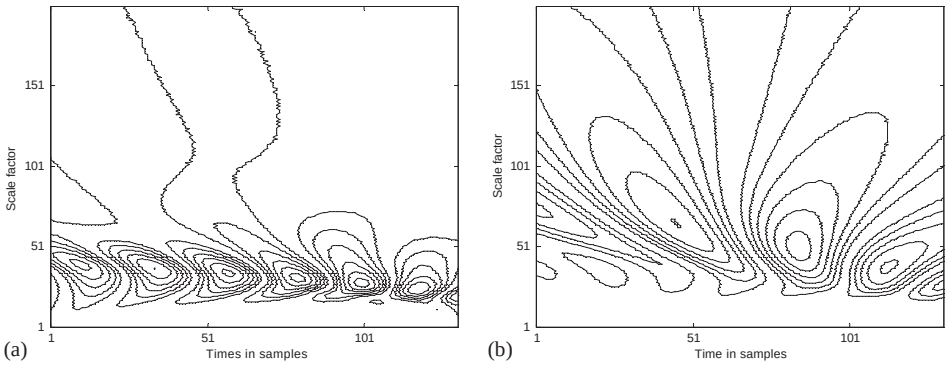

Fig. 10. The influence of the unbalance angle on the wavelet time–frequency feature: (a) $\beta = \pi/2$, (b) $\beta = \pi$.

and the wavelet time–frequency feature still takes on the form of six group circles. To identify the cracked rotor effectively, the unbalance angle should be changed to $\beta = 0$ by balancing technique when the Wigner–Ville distribution is adopted.

6. Conclusions

(1) Based on the simple hinge crack model, the dynamic equation of transient response in a cracked rotor is modelled; the numerical simulation solutions of the cracked and the uncracked rotors are obtained.

(2) The time–frequency features of the cracked and the uncracked rotors obtained by using the Wigner–Ville distribution are compared with those obtained by using the wavelet transform. The Wigner–Ville time–frequency feature of the uncracked rotor takes on the form of regular ellipses, and there exists oscillation in the Wigner–Ville time–frequency feature of the cracked rotor. The wavelet time–frequency feature of the uncracked rotor is characteristic of two group circles due to the unbalance, and the wavelet time–frequency feature of the cracked rotor is characteristic of six group circles due to the crack excitation besides two group circles due to the unbalance. The wavelet transform and the Wigner–Ville distribution can identify the cracked rotor effectively, but to some extent, the wavelet transform is superior to the Wigner–Ville distribution.

(3) The sensitivity of the Wigner–Ville distribution and the wavelet transform to the stiffness variation is investigated, and the wavelet transform is more sensitive to the stiffness variation than the Wigner–Ville distribution.

(4) The influence of the unbalance and the unbalance angle on the Wigner–Ville distribution and the wavelet transform is discussed. Even if the unbalance increases significantly, the Wigner–Ville distribution and the wavelet transform still can identify the cracked rotor. The influence of the unbalance angle on the Wigner–Ville time–frequency feature is great, and the influence on the wavelet time–frequency feature is small.

Acknowledgements

This project is supported by National Fundamental Foundation of Research and Development (approved No. G1998020321), by National Natural Science Foundation and Institute of

Engineering Physics of China (approved No. 10176014), also by the State Key Laboratory of Vibration, Shock and Noise (approved No. VSN-2002-03), the authors are grateful to their financial support.

References

[1] J. Wauer, On the dynamics of cracked rotors: a literature survey, *Applied Mechanics Review* 43 (1990) 13–17.
[2] A.D. Dimarogonas, Vibration of cracked structures: a state of the art review, *Engineering Fracture Mechanics* 55 (1996) 831–857.
[3] R. Gasch, A survey of the dynamic behavior of a simple rotating shaft with a transverse crack, *Journal of Sound and Vibration* 160 (1993) 313–332.
[4] R. Gasch, Dynamic behavior of a simple rotor with cross-sectional crack, IMechE Conference Publication c178/76, London, 1976, pp. 123–128.
[5] A.D. Dimarogonas, C.A. Papadopoulos, Vibration of cracked shafts in bending, *Journal of Sound and Vibration* 91 (1983) 583–593.
[6] A.D. Dimarogonas, S.A. Paipetis, *Analytical Methods in Rotor Dynamics*, Applied Science Publisher, New York, 1983.
[7] C.A. Papadopoulos, A.D. Dimarogonas, Coupled longitudinal and bending vibrations of a rotating shaft with an open crack, *Journal of Sound and Vibration* 117 (1987) 81–93.
[8] S. Ratan, J. Rodriguez, Transient dynamic analysis of rotor using SMAC techniques: Part 1, formulation, *Transactions of American Society of Mechnical Engineers, Journal of Vibration and Acoustics* 114 (1992) 477–481.
[9] S. Ratan, J. Rodriguez, Transient dynamic analysis of rotor using SMAC techniques: Part 2, numerical study, *Transactions of American Society of Mechanical Engineers, Journal of Vibration and Acoustics* 114 (1992) 482–488.
[10] R.H. Plaut, R.H. Andruet, S. Suherman, Behavior of a cracked rotating shaft during passage through a critical speed, *Journal of Sound and Vibration* 173 (1994) 577–589.
[11] A.S. Sekhar, B.S. Prabhu, Transient analysis of a cracked rotor passing through critical speed, *Journal of Sound and Vibration* 173 (1994) 415–421.
[12] A.S. Sekhar, B.S. Prabhu, Condition monitoring of cracked rotor through transient response, *Mechanics and Machine Theory* 33 (1998) 1167–1175.
[13] S. Prabhakar, A.S. Sekhar, A.R. Mohanty, Detection and monitoring of cracks in a rotor-bearing system using wavelet transforms, *Mechanical Systems and Signal Processing* 15 (2001) 447–450.
[14] J. Zou, J. Chen, Y.P. Pu, On the wavelet time–frequency analysis algorithm in identification of a cracked rotor, *Journal of Strain Analysis for Engineering Design* 37 (2002) 239–246.
[15] S.A. Mallat, Theory for multiresolution signal decomposition: the wavelet representation, *IEEE Transactions on Pattern Analysis and Machine Intelligence* 11 (1989) 674–693.
[16] Y. Meyer, *Wavelet Algorithms and Application*, Society for Industrial and Applied Mathematics, Philadelphia, 1993.
[17] J. Zou, J. Chen, Z.M. Geng, Application of wavelet packets algorithm to diesel engines' vibroacoustic signature extraction, *Proceedings of IMechE, Part D, Journal of Automobile Engineering* 215 (2001) 987–994.
[18] Z.M. Geng, J. Chen, J. Zou, On the diesel engine's impulsive-source features extraction, International conference of DYMAC, Manchester, 1999, pp. 101–107.
[19] K. Darowicki, A. Krakowiak, A. Zielinski, The comparative study of different methods of spectral analysis of electrochemical oscillations, *Electrochemistry Communications* 4 (2002) 158–162.
[20] S. Serutti, A.M. Bianchi, L.T. Mainardi, Advanced spectral methods for detecting dynamic behavior, *Autonomic and Neuroscience: Basic and Clinical* 90 (2001) 3–12.
[21] T.A.C.M. Classen, W.F.G. Mecklenbrauer, The Wigner distribution a tool for time–frequency signal analysis: Part I. continuous time signals, *Philips Journal of Research* 35 (1980) 276–350.